IJE TRANSACTIONS C: Aspects Vol. 35, No. 09, (September 2022) 1765-1778

International Journal of Engineering

Journal Homepage: www.ije.ir

The Reliability Assessment of a Ship Structure under Corrosion and Fatigue, using Structural Health Monitoring

M. Sadeghian*

Department of Mechanic Engineering, Malek –e Ashtar University of Technology, Isfahan, Iran

P A P E R I N F O

Paper history:
Received 29 April 2022
Received in revised form 12 June 2022
Accepted 17 June 2022

Keywords:
Corrosion
Fatigue
Reliability
Structural Health Monitoring

A B S T R A C T

Reliability of a ship structure has been investigated in this study under two factors of fatigue and corrosion failure using structural health monitoring data. In order to use structural health monitoring data in assessing the reliability, Bayesian inference method has been used to update the distribution of loads applied on the structure. This study used structural health monitoring data to assess the reliability of a ship construction under two conditions: fatigue and corrosion failure. A Bayesian inference method was utilized to update the distribution of loads applied to the structure to employ structural health monitoring data in determining reliability. The load distribution obtained from the equations was used to assess the reliability of a ship structure during corrosion. The proposed mathematical model was examined using the data output of the force sensors installed on the commercial ship in the laboratory, whose model has been scale tested. According to the reliability analysis, the reliability index of the structure decreases with time as a result of corrosion and fatigue failures. The utilization of structural health monitoring data has boosted confidence in the reliability index for estimating the structure's real-life as determined by the study. The findings suggest that using the reliability criterion and health monitoring data during the design stage can provide a better knowledge of the structure's performance throughout time, according to the environmental conditions.

doi: *10.5829/ije.2022.35.09c.13*

1. INTRODUCTION

It is critical to ensure the safe operation of marine ships as well as the prevention of contamination caused by the destruction of these structures. To accomplish this, a thorough understanding of the ship's structure and the loads applied to it is essential. Because the loads applied to the structure of ships are uncertain, and correct identification of damages generated in the structure is difficult and expensive, it is required to develop a realistic analytical process for the structure. To account for existing uncertainties and give a realistic analysis, the use of probabilistic approaches in the study of engineering structures has increased in recent years. The use of structural reliability analysis methods has increased due to the strength of the structure and the loads applied to it to determine the remaining life, determine the periods of inspection and maintenance at the time of service of the structures, and is becoming a major trend in the study of these structures. Existing uncertainties in structural and loading characteristics are determined using mathematical theories of probabilities, stochastic variables, random and statistical processes. Analysis, design, and optimization of high-risk structures such as nuclear power plants, dams, maritime structures, and other high-risk industries are among the areas of application. The range of structural behavior includes stress analysis, dynamic, deformation control, creep and release, failure, fatigue, and structural stability. Preliminary studies in this field have been conducted by Freudenthal [1] undertook preliminary research in this area, taking into consideration statistical and probabilistic methodologies in characterizing the nature of the reliability index. Engineers and academics have significantly applied reliability estimation and analysis methodologies for structures with defects in pressurized

*Corresponding Author Institutional Email: sadeghian2@aut.ac.ir (M. Sadeghian)

Please cite this article as: M. Sadeghian, The Reliability Assessment of a Ship Structure under Corrosion and Fatigue, using Structural Health Monitoring, ***International Journal of Engineering, Transactions C: Aspects***, Vol. 35, No. 09, (2022) 1765-1778

components with the development of reliability engineering and probabilistic failure mechanics.

By categorizing tasks into random variables, stochastic process reliability analysis models, and stochastic field reliability models, Bjerager [2] presents a case of structural reliability methods.

Cizelj et al. [3] employed first and second-order reliability methodologies, as well as various modeling methods, to assess the safety of steam generator pipes with axial stress corrosion cracking. They calculated data scatter relating to pipe geometry, material parameters, and crack progression using the probabilistic failure mechanics model. They focused on the impact of the maintenance technique and compared the outcomes of real-world numerical examples from each method. Using the supplied formulae for loads applied to the structure, on the other hand, may result in unrealistic analytical results.

As a result, using the findings of structural health monitoring can provide meaningful data to analysts when evaluating the ship structure's performance accuracy. Vibrational methods have a specific place in damage identification among structural health monitoring techniques. Applying these techniques for monitoring structural health, in addition to the possibility of using them during ship operations, can assist in detecting damages early in their development and preventing major structural damage. These techniques rely on sensors and equipment deployed on the structure to extract information from measured signals. The vibrational properties of each structure are unique. As a result, variations in these vibrational qualities imply structural damage. These techniques rely on sensors and equipment deployed on the structure to extract information from measured signals. The vibrational properties of each structure are unique. As a result, variations in these vibrational properties imply structural damage. According to previous study, more than 40% of fatigue-induced failures in ship structures, such as cracks, occur in the side shell of the hulls and at the junction of longitudinal and transverse stiffeners [4].

As a result, studies have been carried out to identify damages caused by fatigue due to cracks in an aluminum stiffener plate in a ship's hull [5] as well as damages caused by corrosion of the ship's hull plate [6, 7]. These damages will increase due to the compressive forces created by the impact of sea waves on the ship's side shell, potentially causing serious damage. Removing a ship from operation for health monitoring or structural repairs is time-consuming and expensive. Therefore, the health of the ship's side shell joints should be monitored continually and throughout operation using methods such as vibration methods and their vibration characteristics, which can vary as a result of damage.

Fatigue failure is also one of the most serious damage events that can occur on a ship [8, 9]. Sea waves and the surrounding environment cause fatigue failure on ships. Estimating a ship's expected life is a difficult and generally ambiguous process. The development of high-strength steel, however, has resulted in the design of ships that can withstand higher stresses. As a result, experts have performed substantial research in this area. With this in mind, Chen et al. [10] have established a relationship between microstructures and fatigue life in steel marine structures. Bea et al. [11] devised and established a method for determining the fatigue life of critical marine ship components. They also examined a set of cracks that had formed on a ship. They discovered that around 40% of the cracks were formed at the intersection of the ship's vertical bulkheads, 10% in the ship's floor bulkheads, and 10% in the ship's transverse stiffeners, out of a total of 3,600 cracks. Many cracks in marine ships originate at the intersection of the ship's vertical walls and transverse bulkheads in general. These locations are subjected to the most dynamic loads [12].

Currently, extensive activities have been performed related to the reliability-based design in the field of the ship structure reliability assessment [13]. Based on the moments given to both calm water and waves, Akpan et al. [14] computed the ultimate strength of the ship's middle section. They evaluated their model for corrosion and fatigue-induced cracking, as well as estimating structural reliability under random loads. Liu et al. [15] used data from structural health monitoring systems in conjunction with a failure mechanics technique based on S-N diagrams to estimate and analyze reliability using probabilistic distribution functions to estimate the ship's lifespan under fatigue-induced damage. Based on structural uncertainties, statistical data and S-N diagrams were utilized to assess longevity and reliability.

Okasha et al. [16, 17] assessed the reliability and damage detection of a fast mono-hull ship based on structural health monitoring. By integrating the information obtained from structural health monitoring through Bayesian method, they determined the reliability of the structure under the uncertainties exist in a ship considering corrosion-induced damage. Deco et al. [18] evaluated the reliability of the ship structure based on the initial and ultimate failure in different sea forces. Kwon and Frangopol [19, 20] evaluated the reliability of a ship structure under simultaneous corrosion and fatigue failures. In this study, they presented their results on stormy sea forces as well as various damage scenarios. Also, assessed and estimated the life cycle of the fast ship structures under fatigue-induced damages. In this study, fatigue and its due failure are presented based on the S-N failure criterion using the model test results in the pond. Zayed et al. [21] evaluated the stability of a ship structure under static moments caused by calm water and wave-induced moments. The employment of rapid techniques has been addressed in this study to calculate moments and section modulus of a commercial ship under the uncertainties imposed by the ship's geometry.

Zhu et al. [22] used information and data generated by health monitoring systems to evaluate the structural reliability of three different sections of big and commercial ships and analyzed the structural reliability under different sea forces.

Campanile et al. [23] investigated the reliability of a cargo ship in both intact and damaged states under a pure moment. In this study, the second-order reliability method was used to estimate the reliability under corrosion-induced damage. Doshi et al. [24] have investigated the reliability of a large cargo ship with a failure mechanics approach under the uncertainties of the ship structure. They used a Bayesian method to update the forces applied to the ship.

In this study, the reliability assessment of the ship structure is reported, using structural health monitoring data under the two damage factors of fatigue and corrosion. A Bayesian inference method was utilized to update the distribution of loads applied to the structure to implement the structural health monitoring data. The proposed mathematical model is studied and analyzed using the data output of the force sensors installed on the commercial ship in the laboratory, whose model has been scale tested. The planned ship's reliability under corrosion and fatigue damage, as well as the existing uncertainties, demonstrates that the structure's reliability will decrease with time.

2. THEORY

2. 1. The limit State of Ultimate Resistance (Range of Strength)

The ship hull risk assessment requires the determination of the limit resistance function with respect to the ship hull structure. The ship hull consists of a continuous and integrated girder under transverse load caused by still water without considering the waves. The model governing the ultimate resistance state can be calculated from the following Equation (1) [14]:

$$g(t) = U(t) - M_L(t) \tag{1}$$

where U (t) is the ship's ultimate resistance capacity model and $M_L(t) is$ the external load effect model on the ship. The overall resistance capability of a ship's hull is reduced due to the wear of the ship's hull over time. The vertical bending moment parameters, which include the hull curvature, are specified in Equation (3). Random functions 2 and 3 define the final failure function of the primary carrying girder.

$$U(t) = M_u(t) \tag{2}$$

$$M_L(t) = M_{sw}(t) + k_w[M_w(t) + k_D + M_{Dyn}(t)] \tag{3}$$

where M_u is the ultimate capacity of the bending moment of the main beam, M_{sw} shows the bending moment resulted from the still water surface, M_w is the bending moment caused by the wave, k_D is the correction coefficient between the bending moment of the wave and the dynamic bending moment, M_{Dyn} indicates dynamic bending moment. k_w is the correlation coefficient that depends on the bending due to stress in the sagging state or stress in the hogging state [25, 26].

2. 2. Fatigue Assessment and Analysis Methods

There are two fundamental approaches for determining a structure's fatigue life:

1. Using lab data (such as the stress-life method or strain-life method) ,
2. Using the failure mechanics method (Paris law),

Stress-life or strain-life methods are prepared by performing several tests on the connection with specific details under intermittent loads with a high number of repetitions (the required number of repetitions for fatigue failure) at a specified stress level, whereas in the failure mechanics method, the crack growth rate in an existing defect and its development are taken into account.

2. 2. 1. S-N Diagram Method in Reliability Assessment

The S-N diagram method is considered the baseline strength and estimates the crack starting from a critical component of the structure as a function of some stress cycles. To perform this, the Palmgren-Miner rule (usually a linear sum) is applied [27]. The S-N curve is determined experimentally based on the type of material and the type of structure (geometry, direction, and welding quality), environmental conditions (air, corrosion, or cathodic protection), and by using linear regression analysis of the test results for a given confidence interval [28, 29].

$$\Delta S = \left(\frac{K}{N}\right)^{\frac{1}{m_f}} \tag{4}$$

where ΔS is the stress changes, N shows the number of cycles required for fatigue failure with a constant double value of the stress amplitude, m_f is the negative slope of the S-N curve, plotted on the log-log diagram, and K is the S-N curve parameter for a given confidence interval. Damage can be written as Equation (5):

$$D = \frac{N_s}{K} E[\Delta S^{m_f}] \tag{5}$$

where N_s is the total number of cycles during the operation time and $E[\Delta S^{m_f}]$ is the expected or mean value of ΔS. the long-term density probability function of the stress amplitude can be evaluated with respect to the local load using the Weibull distribution [30, 31]:

$$f(\Delta S) = \frac{\zeta}{W}\left(\frac{\Delta S}{W}\right)^{\zeta-1} \exp\left(-\frac{\Delta S}{W}\right)^{\zeta} \tag{6}$$

where ζ is the shape factor, W is the scale factor, and ΔS shows the stress changes. Thus, considering Weibull distribution, the amount of stress amplitude is:

$$S_{re} = E[\Delta S^{m_f}] = W^{m_f}\Gamma\left(1+\frac{m_f}{\zeta}\right) \quad (7)$$

Also, the mean value of the stress amplitude can be obtained according to the relation provided by Miner [19]:

$$S_{re} = \left[\sum \frac{n_i}{n_{total}} S_{ri}^{m_f}\right]^{\frac{1}{m_f}} \quad (8)$$

where n_i is the number of cycles in stress amplitude. According to the changes of the occurrence probability according to the sea forces and the speed of the ship, it can be written [19]:

$$S_{re}^{*} = \left[\sum_{i=1}^{ss}\sum_{j=1}^{sp}\sum_{k=1}^{wh} P_{SS.i}P_{SP.j}P_{WH.k}S_{re.ijk}^{m}\right]^{\frac{1}{m}} \quad (9)$$

where $P_{SS.i}$ is the occurrence probability at ith sea forces, $P_{SP.j}$ shows the occurrence probability in jth velocity, and $P_{WH.k}$ is the occurrence probability in kth wave of the forecastle. Also, for the number of cycles, we have:

$$N_{avg}^{*} = \left[\sum_{i=1}^{ss}\sum_{j=1}^{sp}\sum_{k=1}^{wh} P_{SS.i}P_{SP.j}P_{WH.k}N_{avg.ijk}\right]^{\frac{1}{m}} \quad (10)$$

Finally, the number of annual cycles is equal to:

$$N(y) = N_{avg}^{*}\alpha 365y \quad (11)$$

where α coefficient expresses the service percentage by the ship at sea (α = 50% .75% .90%). ultimately, the limit state function is extracted to evaluate the reliability based on the S-N curve, as Equation (12) [32]:

$$g(t) = \Delta - D(t) \rightarrow g(t) = \Delta - \frac{N(y)}{K}E[\Delta S^{m_f}] \quad (12)$$

2. 3. Corrosion Assessment and Analysis Methods

Ship structure oldness overtime result to decrease of final strength capacity. The Equation (1)is specified the vertical bending moment parameters such as hull bending. Final bending moment capacity of hull girder is calculated by Equation (13) [14]:

$$M_u(t) = \phi\sigma_u Z(t) \quad (13)$$

That ϕ non-dimensional factor known as buckling knock down factor, σ_u ultimate strength of the ship hull cross section and $Z(t)$ is the midship hull elastic section modulus. In cases where a relationship between damage, such as fatigue crack and corrosion, and σ_u can be established, σ_u should be replaced with that relationship. It is well known that structural degradations will affect the hull girder capacity by reducing the section modulus $Z(t)$ depends on time. The impact of the degradation mechanisms and the modeling strategies that are adopted herein are presented in the following sections. The buckling knock down factor is of high variability and depends on the ship type or class and the location of a section.

Corrosion decreases the section modulus of the ship hull structure by thinning the thickness of primary structural members and also it reduces the ability of the structure to resist the externally induced bending moment. Some several models of general corrosion growth have been suggested [33]. The current model in this paper is the Equation (14) [14].

$$r(t) = C_1(t-t_0)^{C_2} \quad (14)$$

where $r(t)$ is thickness decreasing rate, t_0 is the life of coating by year, t is the age of the vessel by year, C_1 and C_2 are coefficients of random variables. C_1 represents rate of annual corrosion and although C_2 can take values ranging from 1/3 to 1. The life of coating varies for different vessels and depends on the coating type [14]. Thus the moment capacity is given by:

$$M_u(t) = \phi\sigma_u \begin{bmatrix} Z(r(t_0)) & t \le t_0 & r(t_0) = 0 \\ Z(r(t)) & t \le t_0 & r(t) = 0 \end{bmatrix} \quad (15)$$

According to Equation (15) $Z(t)$ is presented as collected data from Figure 1, prediction equation for reducing of hull girder section module compare to initial amounts bring at Table 1.

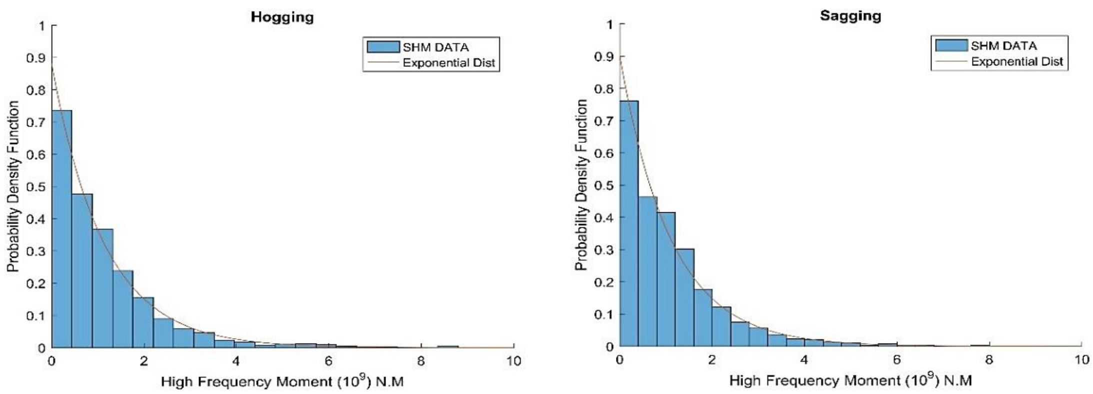

Figure 1. Histogram and probability density function for high frequency moments in sagging and hogging modes

TABLE 1. The equation of prediction mean amount and reducing of hull girder section module standard deviation [34]

Amount	Reducing of hull girder section module	Year
mean	$R_m(t) = \frac{0.62(t-6.5)^{0.67}}{100}$	$t > 6.5$
mean + standard deviation	$R_{m+\sigma}(t) = \frac{0.8(t-5)^{0.75}}{100}$	$t > 5$
Standard deviation	$R_{m+\sigma} = R_{m+\sigma}(t) - R_m(t)$	$t > 6.5$

The replacement of mean amount equation plus standard deviation at Equation (15) concluded to main hull girder bending moment capacity.

$$M_u(t) = x_u \phi \sigma_u S_m \left[1 - \left(0.8\frac{(t-5)^{0.75}}{100}\right)\right] \tag{16}$$

where x_u is the random variable representing modeling uncertainty in ultimate strength and S_m is main or initial hull girder bending moment capacity [34].

2. 4. Bayesian Theory and Inference Method

Bayesian theory can also be generalized from discrete to continuous problems. Assuming that a set of parameters (θ Must be inferred, all current knowledge of these parameters is represented by $f'(\theta)$, which is called the prior distribution. The choice of the prior distribution type reflects the perceptual knowledge associated with the uncertainty of the parameter before observing the new event. In fact, it is assumed that this distribution has the ability to explain the data with some degrees of uncertainty. Measuring observed data (D) has been done on a value corresponding to (θ). This information can be used to update the distribution (θ) to achieve the posterior distribution $f''(\theta)$ as follows [35]:

$$f''(\theta) = \frac{L(\theta)f'(\theta)}{\int L(\theta)f'(\theta)d\theta} \tag{17}$$

In the above relation, $L(\theta)$ is the likelihood function θ, which is proportional to the probability $P(D|B)$, and is equal to the probability of observing the data D under the condition θ. The denominator to the right of the above relation is equal to a normalizing constant value which is called normalizer. According to this constant, the above relation is represented as Equation (18) [22]:

$$f''(\theta) \propto L(\theta)f'(\theta) \tag{18}$$

Using the law of total probability of the posterior predictive distribution for the variable x are calculated on the basis of the updated variables in Equation (19).

$$f'_X(x) = \int_{-\infty}^{\infty} f_x(x|\theta)f''(\theta)d\theta \tag{19}$$

In the current study, the posterior distribution has a log-normal distribution. The univariate log-normal distribution is equal to [36]:

$$f(\mu_n) = \frac{1}{\zeta \mu_n \sqrt{2\pi}} exp\left[-0.5\left(\frac{ln\mu_n - \lambda}{\zeta}\right)^2\right] \tag{20}$$

where λ and ζ are the parameters of the log-normal distribution and are calculated as Equation (21):

$$\zeta = \sqrt{ln\left(1 + \frac{\sigma^2}{\mu^2}\right)} \qquad \lambda = ln\,\mu - 0.5\zeta^2 \tag{21}$$

Also, for two-variable log-normal distribution, it can be written [22, 36]:

$$f(\mu_n.\alpha_n) = \frac{1}{2\pi\zeta_1\zeta_2\sqrt{(1-\rho^2)}} * \frac{1}{\mu_n\alpha_n} * exp\left(-\frac{1}{2(1-\rho^2)}(A^2 - 2\rho AB + B^2)\right) \tag{22}$$

For A and B, we have:

$$A = \frac{\log(\mu_n) - \lambda_1}{\zeta_1} \qquad B = \frac{\log(\alpha_n) - \lambda_2}{\zeta_2} \tag{23}$$

Also, λ_1, λ_2, ζ_1 and ζ_2 are distribution parameters. The likelihood distribution in current study has a final value distribution (extreme value theory) of the first kind. For this distribution you can write [35]:

$$f_{Y_n} = \frac{1}{\alpha_n} exp\left(-\frac{(y-\mu_n}{\alpha_n}\right) exp\left(-\exp\left(-\frac{(y-\mu_n}{\alpha_n}\right)\right) \tag{24}$$

where μ_n and $\alpha_n$are Farin distribution parameters. Also, the relation between theses parameters and standard deviation is equal to:

$$\mu = \mu_n + 0.57721\alpha_n \qquad \sigma = \frac{\alpha_n \pi}{\sqrt{6}} \tag{25}$$

2. 5. Reliability Assessment

Based on the reliability theory, the limit state function can be defined based on the difference between stress (load) and resistance [29, 37].

$$g(t) = R - S \tag{26}$$

where $g(t)$ is the limit state function, R is resistance and R shows stress or applies load. If $g(t) \geq 0$, the operation of the structure can be in the safe margin, but if $g(t) \leq 0$, it indicates the failure range. The probability of failure is expressed as follows:

$$P_F = P(L(t) < 0) \tag{27}$$

Given the complexity of Equation (27), it will be very difficult to evaluate and analyze the equation. Therefore, in order to evaluate and analyze in this case, the reliability index assessment method can be used.

3. APPLICATIONS

3. 1. The Model under Study In this study, health monitoring data, which was scale-tested by body-mounted sensors in the laboratory, was used to assess reliability [38]. The specifications of the middle section of the ship in study for the implementation of reliability evaluation calculations is shown in Table 2. Auther used data from the ship's middle section, which included 21 tests at a speed of 35 knots, a temperature of 0°, and seven sea forces. Each test consisted of approximately 3200 to 4000 samples. There were 73,800 data points in total. The sample rate was set to 200 HZ. The duration of the test was around 6.15 minutes. All data was converted, taking into account the landing scale factor in the ship's actual dimensions. Bending moment, time and modulus of section were converted with the scales of $1.025\lambda^4$, $\sqrt{\lambda}$ and $0.346\lambda^4$, respectively. The measured time of the full-scale experiment was 42.28 minutes. The signals obtained from the structural health monitoring in the middle section of the ship are filtered and the high and low-frequency waves are separated. A developed extraction algorithm has been used to extract the maximum moments obtained from the wave cycle [38].

3. 1. 1. Middle Section Resistance Modeling The bending strength for the initial failure and the ultimate flexural bending strength are calculated. For this purpose, the calculations are conducted according to the random variables, t plate thickness, E elasticity modulus, σ_{yp} yield stress, and σ_{ys} stiffener yield stress which have a log-normal distribution with COV of 0.05, 0.03, 0.1 and 0.1, respectively. The amount of residual stress is also considered equal to 5% of the plate yield stress. For each sample, the initial and ultimate bending moments of the failure are calculated and the results of the total moments in each case are used for fitting the probability distribution. This has been repeated for 30 years over a period of 2 years, each time the web thickness and the flange stiffener has increased due to the decrease in thickness caused by corrosion over time. Table 3 shows the standard deviation and the mean annual normal log corrosion rate assumed for parameter C1 relative to the location of the stiffener plate.

3. 1. 2. High-frequency Waves Modeling The choice of exponential distribution can be criticized since its value in the most probable case is zero. In fact, for evaluation and design, the obtained results require extrapolation to distribute the final values. The values obtained for the two modes of sagging and hogging are presented in Table 4.

3. 1. 3. Calculating the Previous Loads The bending moment due to still and wavy water has been calculated using the equations provided by the International Association of Classification Societies (IACS (95)) [39, 40]. The change of these moments is calculated by considering the moment caused by still water and the bending moment caused by the wave with normal distribution and the first kind of final value with COV equal to 0.15 for both moments. A summary of these results is shown in Table 5.

3. 2. Updating Parameters

3. 2. 1. Structural Reliability Assessment Considering Previous Loads The reliability of the middle section of the ship is assessed for two modes of sagging and hogging over a period of 30 years. For this purpose, the reliability of the structure has been evaluated using Equation (3). The specifications of the parameters are presented in Table 6.

TABLE 2. Geometrical profiles of the components [38]

Stiffener number	Stiffener plate height $d(mm)$	Stiffener plate thickness $t_w(mm)$	Stiffener plate width $b(mm)$	Flange plate thickness $t_f(mm)$
1	125.5	4.4	100.6	5.3
2	200.4	4.3	100.1	5.2
3	250.7	4.8	100.6	5.3
4	206	6.2	102.1	8
5	304.5	5.6	101.3	6.7
6	308.9	6	101.9	8.9
7	258.3	6.1	146.1	9.1
8	349	5.8	127	8.5
9	204.7	7.2	166.1	11.8
10	173.5	7.7	203.2	13.5
11	616.7	13.2	230.1	22.1
12	616.2	14	325.1	21.6
13	628.4	16.5	327.7	27.7
14	911.4	19.6	418.3	32

TABLE 3. Parameter C1 for corrosion model in different parts of the ship [17]

Location	Mean (mm/year)	Standard deviation (mm/year)
Deck plates	0.008125	0.000406
Deck stiffeners	0.008125	0.000406
Wall plates	0.003750	0.000188
Wall stiffeners	0.003750	0.000188
Ship floor plates	0.021250	0.001063
Ship floor stiffeners	0.008125	0.000406

TABLE 4. The final value distribution parameters for high-frequency loads

Loading parameter	Mean $(\mathbf{N \cdot M})$	Coefficient of variation	Distribution
Sagging	1.183*e+9	0.134	First kind final value
Hogging	1.185*e+9	0.134	First kind final value

TABLE 5. Statistical description and distribution of previous applied loads

Loading parameter	Mean $(\mathbf{N \cdot M})$	Coefficient of variation	Distribution
Sagging for still water	1.823*e+9	0.15	Normal
Sagging for wave	3.867*e+6	0.15	First kind final value
Hogging for still water	3.283*e+9	0.15	Normal
Hogging for wave	2.729*e+9	0.15	First kind normal value

TABLE 6. Random parameters specifications

Variable	Mean	COV	Distribution
$\boldsymbol{x_u}$	1	0.1	Normal
$\boldsymbol{x_{sw}}$	1	0.05	Normal
$\boldsymbol{x_w}$	0.9	0.15	Normal
$\boldsymbol{k_d}$	1	-	-
$\boldsymbol{M_{sw}}$	μ	0.15	Normal
$\boldsymbol{M_w}$	μ	0.15	First kind final value

The reliability index has been calculated based on previous data. Also, the strength of the structure is considered for the both initial and ultimate failure modes. The reliability index obtained from the analysis with respect to the previous data is shown in Figure 2.

As can be seen, reliability reduces over time because of the increase in the corrosion rate as well as considering the fact that the loads applied to the structure are constant due to the effect of corrosion. The amount of reliability index in the initial failure mode is less than the ultimate failure, because in the initial failure made, our criterion is the failure of the first component. In Hogging mode, the slope of decreasing the reliability index is higher, which can be attributed to the magnitude of wave loads in hogging mode and its incremental effect in this mode.

3. 2. 2. Time-dependent Reliability The final strength of the ship hull M(u) decreases with time in the presence of fatigue mechanisms; thus, the probability of failure is also a function of time. By changing the period t from 0 to 1, the expected service life, the amount of final strength reduction can be estimated. Therefore, the probability of instantaneous failure at a time t, can be deduced regardless of the ship's conditions in the past, using Equation (28). However, the successive annual loads and annual values, the reduction of the final strength of the ship, are interdependent and must be taken into account to estimate the reliability. This is done using advanced or time-dependent reliability estimates based on conditional probability theory. For continuous systems, the hazard rate is defined by Equation (28) [41].

$$h(t) = \frac{P_f(t_i)}{1-\sum_{j=1}^{i=1} P_f(t_i-1)} \quad (28)$$

where $P_f(t_i)$ is the failure probability at ith time. The value of the probability of instantaneous and time-dependent failure is shown in Figure 3.

3. 2. 3. Updating Parameter μ_n Loading data is updated considering previous loads and results obtained from structural health monitoring. For this purpose, the data is updated using the Bayesian inference method. In this research, first, the parameter μ_n of the final value distribution is considered as the desired parameter for updating the load distribution. The MCMC method has also been used to approximate this parameter with respect to Bayesian inference. The parameter μ_n is presented as a variable with a log-normal distribution whose mean is equal to the value of the prior distribution and its standard deviation with respect to COV is equal to 10%. The results obtained from updating the parameter μ_n are shown in Figure 4.

According to Figure 4, it can be seen that after updating μ_n, the mean of μ_n has decreased in both sagging and hogging modes. The loading distribution is evaluated according to the parameter μ_n update (Figure 5).The reliability index was calculated according to the main load distribution without considering the data obtained from structural health monitoring in the previous section, which is again presented in the following Figure. By updating the load and considering the structural health monitoring data in evaluating the reliability index, which includes low- and high-frequency loads, the reliability index was evaluated in this case and compared with the previous case (Figure 6).

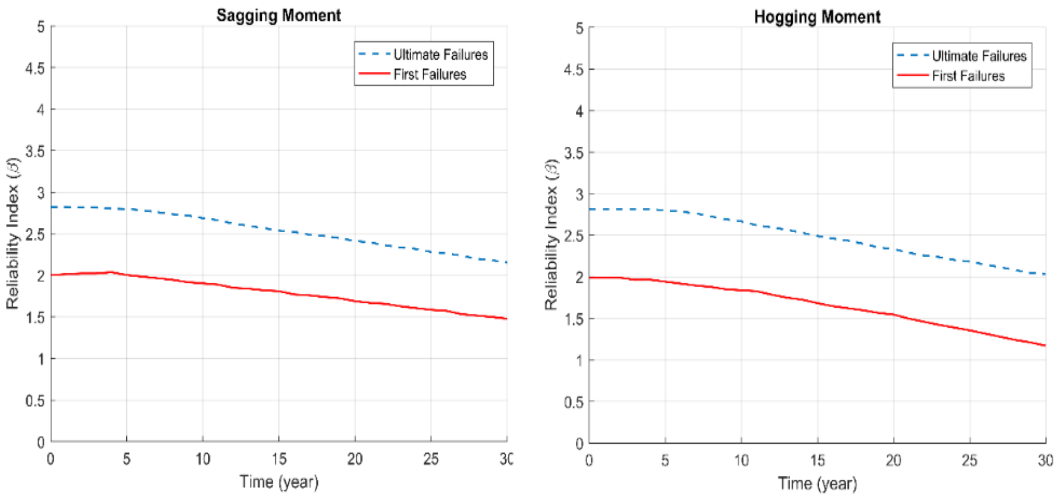

Figure 2. Reliability index considering previous loads in sagging and hogging modes

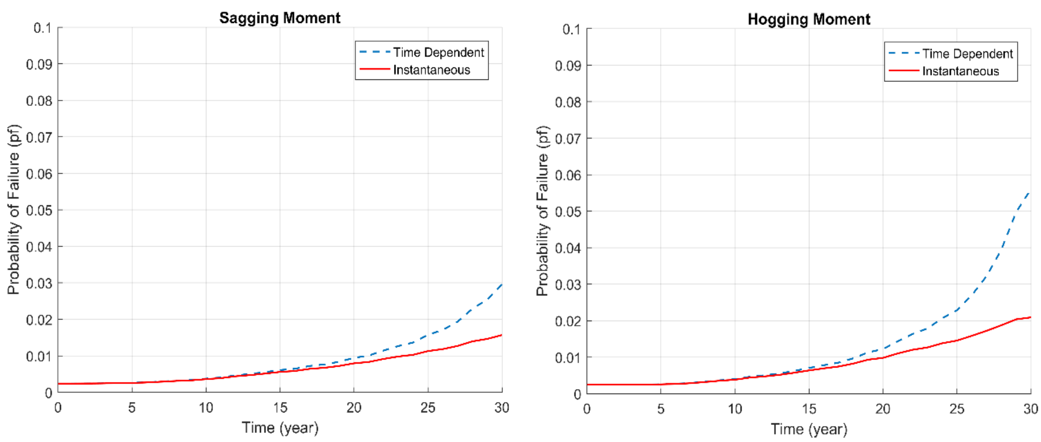

Figure 3. The probability of instantons and time-dependent failure

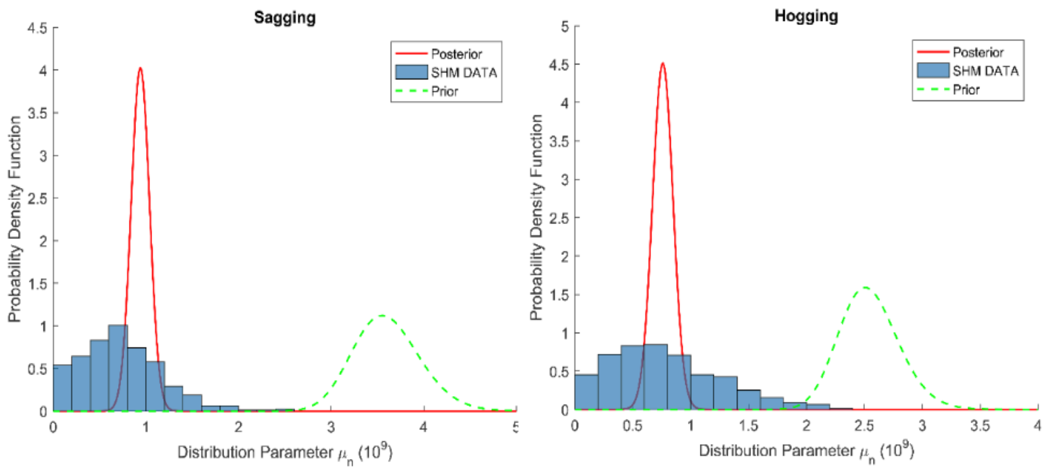

Figure 4. Updated Bayesian results for the parameter μn in both sagging and hogging modes

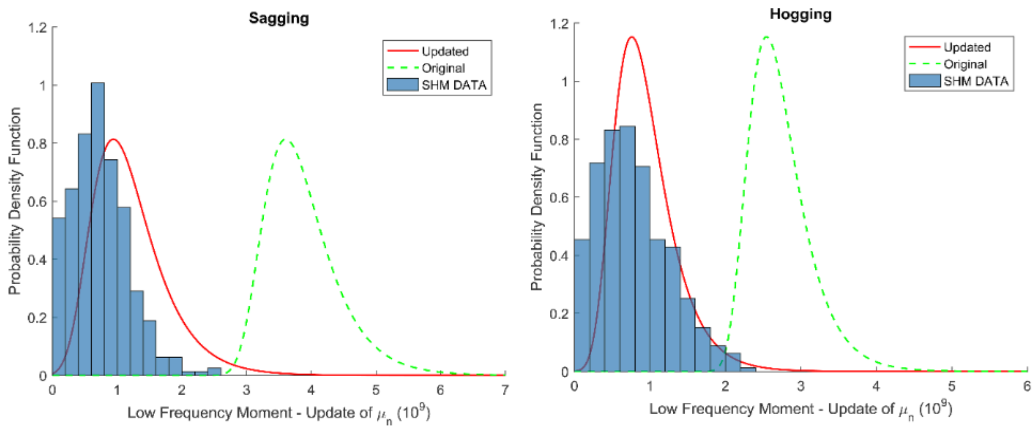

Figure 5. Main and updated loading distributions in both sagging and hogging modes according to μ_n update

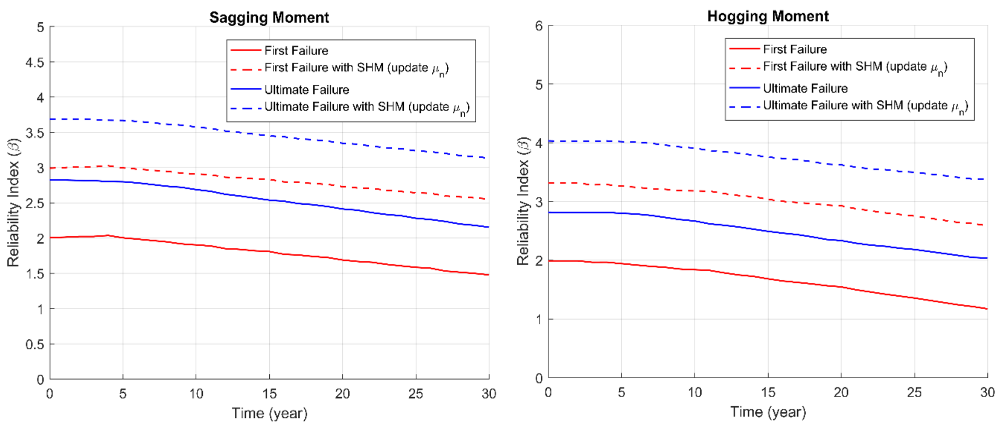

Figure 6. Reliability index evaluated according to previous data and parameter μ_n update

3. 2. 4 Updating Parameter α_n The parameter α_n of the final value distribution with the log-normal distribution has been updated, whose mean is equal to the value of the prior distribution and its standard deviation is 10% with respect to COV. The updated distribution of the parameter α_n is shown in Figure 7.

According to Figure 7, it can be seen that the value of the parameter α_n has increased after the update. Also, the main load distribution and the updated distribution according to the α_n update are presented in Figure 8.

According to Figure 8, it can be seen that after updating α_n. the updated loading distribution has a mean equal to the main distribution, but its standard deviation has increased. It shows that loading uncertainty has increased by considering the parameter α_n as the update criterion. The reliability index is shown in Figure 9 with respect to the main and updated loading distribution.

According to Figure 9, it can be seen that after updating α_n, the reliability index has decreased sharply, which is due to the increase in standard deviation (increase in distribution range) and the stability of the mean of distribution.

3. 3. Reliability Assessment of Fatigue The reliability index of the ship is assesses considering data obtained from the structural health monitoring using Equation (4) to (12) and (3) values of α (0.5, 0.75, and 0.9). According to the Figures 10 and 11 are illustrated above, it can be seen that the probability of fatigue failure increases over time as well as with an increase in the value of α.

3. 4. Reliability of the Ship under Simultaneous Fatigue and Corrosion Damages The simultaneous impact of these two phenomena on the reliability of the ship has been evaluated. The results are presented in Figure 12.

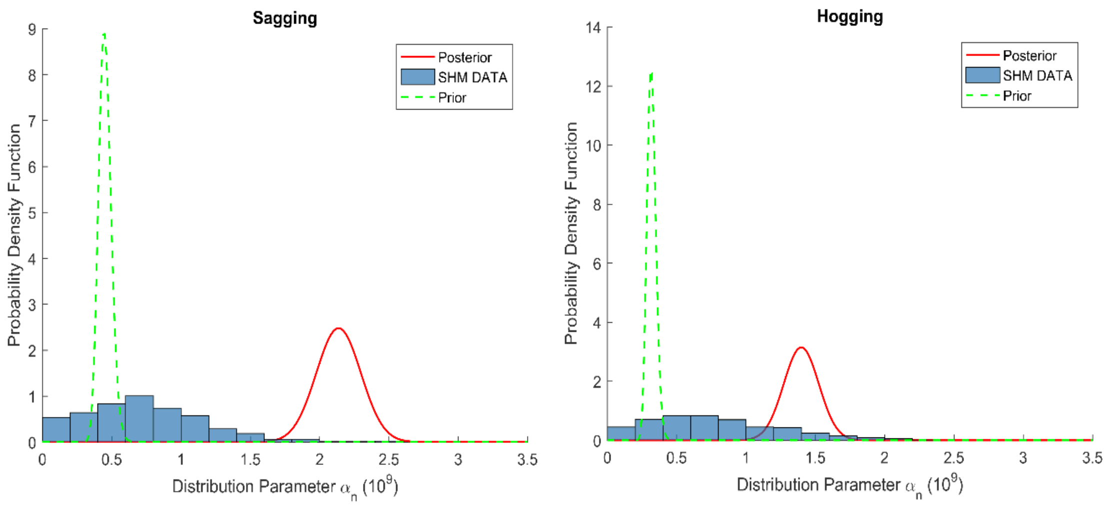

Figure 7. Updated Bayesian results for parameter α_n in both sagging and hogging modes

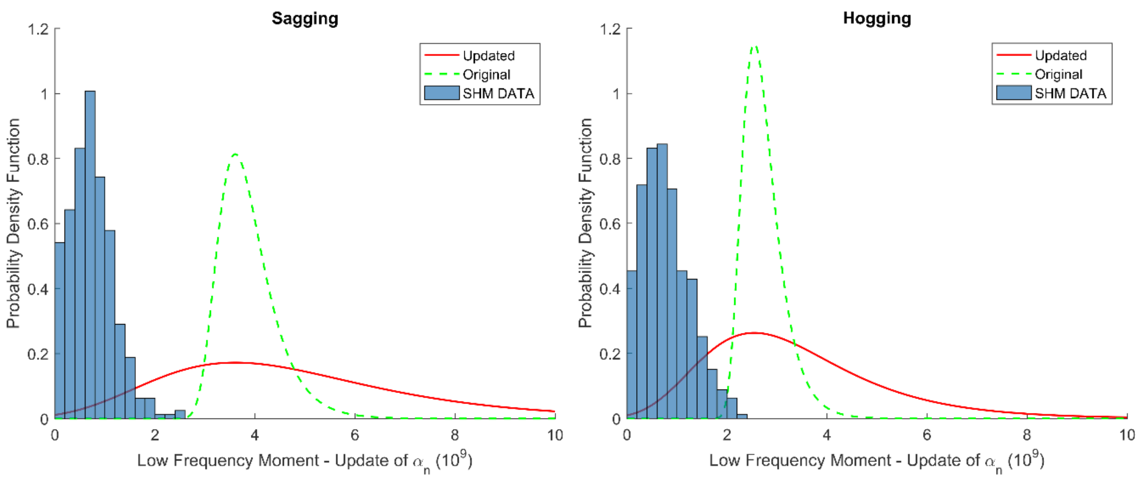

Figure 8. Main and updated distributions of loading in both sagging and hogging modes according to α_n update

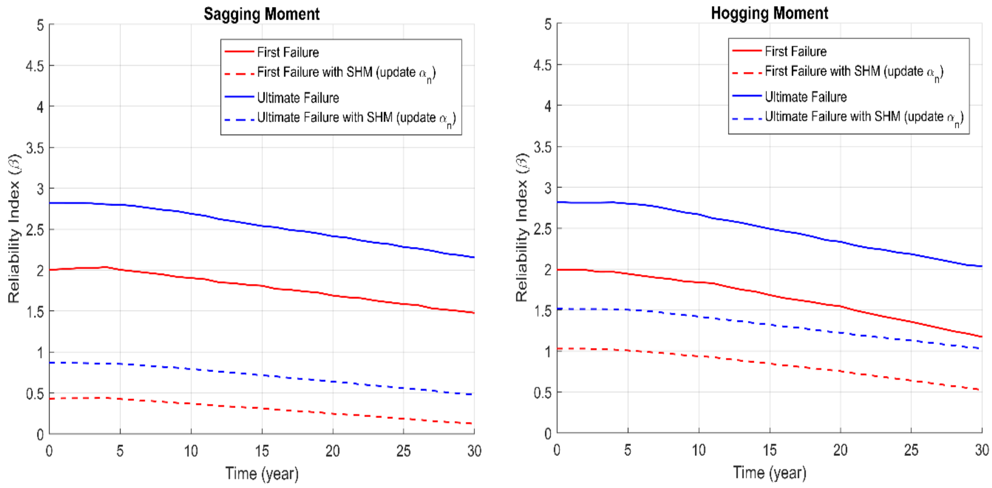

Figure 9. Reliability index assessed with respect to the previous data and parameter α_n update

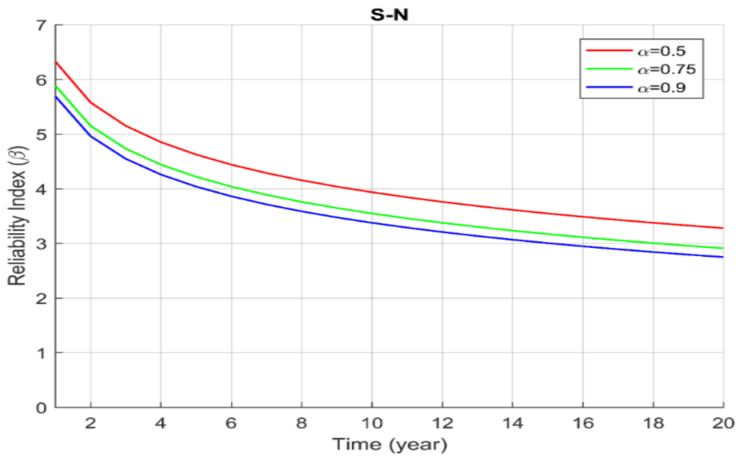

Figure 10. Reliability index of the ship versus fatigue failure considering data obtained from the structural health monitoring

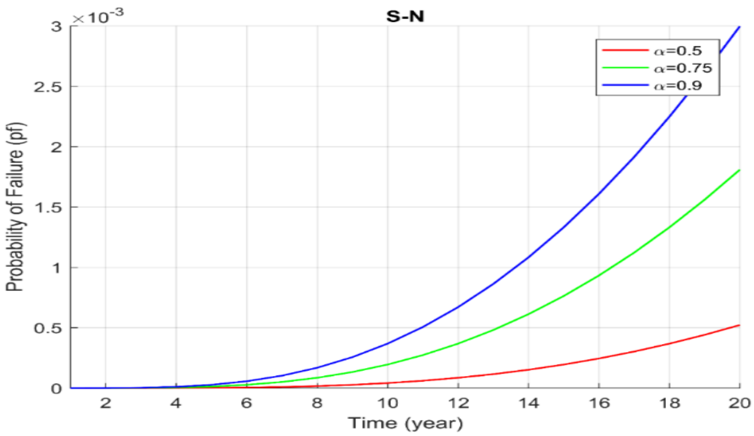

Figure 11. Failure probability of the ship versus fatigue failure considering data obtained from the structural health monitoring

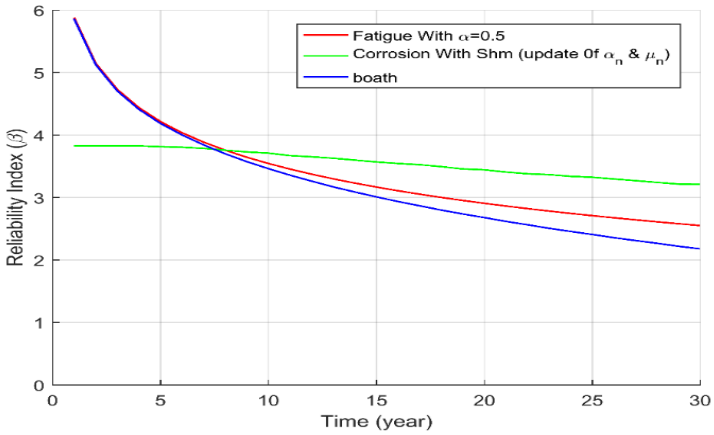

Figure 12. Reliability of the ship under the impact of fatigue, corrosion (in hogging mode) and the simultaneous impact of fatigue and corrosion

4. CONCLUSION

The reliability assessment of the ship structure is expressed under two factors: fatigue and corrosion failures-using structural health monitoring data on a commercial ship. In order to use structural health monitoring data in assessing reliability, a Bayesian inference method has been used to update the distribution of the loads applied to the structure. Given the distribution of the loads obtained from the equations in initial and ultimate failure modes, the reliability of the structure shows that considering the initial failure as an analysis criterion can lead to conservative results. The mean value of the distribution of the loads applied to the structure of the ship is decreased after updating $\boldsymbol{\mu_n}$ and $\boldsymbol{\alpha_n}$ parameters, and the value of the standard deviation of the distribution is updated and slightly increased. It leads to an increase in reliability in relation to the first case. The reliability index obtained from the structural fatigue analysis shows that in the early years of service, the ship has a very high-reliability index, but over time it has decreased sharply. Comparing the reliability index obtained from fatigue analysis with corrosion analysis shows that structural fatigue can be very dangerous, because the reliability index obtained from fatigue analysis is reduced over time with a very steep slope compared to the reliability index obtained from corrosion analysis. Also, the evaluation of the reliability index of the structure indicates that the simultaneous corrosion and fatigue damages increase the downward slope of the reliability index over time.

5. REFERENCES

1. Freudenthal, A.M., "The safety of structures", ***Transactions of the American Society of Civil Engineers***, Vol. 112, No. 1, (1947), 125-159, doi: 10.1061/TACEAT.0006015.
2. Bjerager, P., "On computation methods for structural reliability analysis", ***Structural Safety***, Vol. 9, No. 2, (1990), 79-96, doi: 10.1016/0167-4730(90)90001-6.
3. Cizelj, L., Mavko, B. and Riesch-Oppermann, H., "Application of first and second order reliability methods in the safety assessment of cracked steam generator tubing", ***Nuclear Engineering and Design***, Vol. 147, No. 3, (1994), 359-368, doi: 10.1016/0029-5493(94)90218-6.
4. Zubaydi, A., Haddara, M. and Swamidas, A., "Damage identification in a ship's structure using neural networks", ***Ocean Engineering***, Vol. 29, No. 10, (2002), 1187-1200, doi: 10.1016/S0029-8018(01)00077-4.
5. Kurata, M., Lynch, J.P., Law, K.H. and Salvino, L.W., Bayesian model updating approach for systematic damage detection of plate-type structures, in Topics in model validation and uncertainty quantification, Vol. 4, (2012), Springer.85-94.
6. Stull, C.J., Earls, C.J. and Koutsourelakis, P.-S., "Model-based structural health monitoring of naval ship hulls", ***Computer Methods in Applied Mechanics and Engineering***, Vol. 200, No. 9-12, (2011), 1137-1149, doi: 10.1016/J.CMA.2010.11.018.
7. Dong, Y., Garbatov, Y. and Soares, C.G., "Strain-based fatigue reliability assessment of welded joints in ship structures", ***Marine Structures***, Vol. 75, (2021), 102878, https://doi.org/10.1016/j.marstruc.2020.102878.
8. Zhao, W., Leira, B.J., Feng, G., Gao, C. and Cui, T., "A reliability approach to fatigue crack propagation analysis of ship structures in polar regions", ***Marine Structures***, Vol. 80, (2021), 103075, https://doi.org/10.1016/j.marstruc.2021.103075.
9. Silva-Campillo, A., Suárez-Bermejo, J. and Herreros-Sierra, M., "Design recommendations for container ship side-shell structure under fatigue strength assessment", ***Ocean Engineering***, Vol. 246, (2022), 110655, https://doi.org/10.1016/j.oceaneng.2022.110655.
10. Chen, N.-Z., Sun, H.-H. and Soares, C.G., "Reliability analysis of a ship hull in composite material", ***Composite structures***, Vol. 62, No. 1, (2003), 59-66, doi: 10.1007/s00773-007-0258-5.
11. Bea, R., Pollard, R., Schulte-Strathaus, R. and Baker, R., "Structural maintenance for new and existing ships: Overview, fatigue cracking and repairs", in Proceedings of the Marine Structural Inspection, Maintenance and Monitoring Symposium, II-A., (1991), 1-25.
12. Bea, R., Cramer, E., Schulte-Strauthaus, R., Mayoss, R., Gallion, K., Ma, K., Holzman, R. and Demsetz, L., "Ship's maintenance project", Conducted at University of California, Berkeley for US Coast Guard/Ship Structure Committee (SSC), SSC-386, (1995).

13. Mansour, A., Wirsching, P., Luckett, M. and Plumpton, A., *Assessment of reliability of existing ship structures*. 1997, DTIC Document.
14. Akpan, U.O., Koko, T.S., Ayyub, B. and Dunbar, T.E., "Risk assessment of aging ship hull structures in the presence of corrosion and fatigue", ***Marine Structures***, Vol. 15, No. 3, (2002), 211-231, doi: 10.1016/S0951-8339(01)00030-2.
15. Liu, M., Frangopol, D.M. and Kwon, K., "Fatigue reliability assessment of retrofitted steel bridges integrating monitored data", ***Structural Safety***, Vol. 32, No. 1, (2010), 77-89, doi: 10.1016/j.strusafe.2009.08.003.
16. Okasha, N.M., Frangopol, D.M., Saydam, D. and Salvino, L.W., "Reliability analysis and damage detection in high-speed naval craft based on structural health monitoring data", ***Structural Health Monitoring***, Vol. 10, No. 4, (2011), 361-379, doi: 10.1177/1475921710379516.
17. Okasha, N.M., Frangopol, D.M. and Decò, A., "Integration of structural health monitoring in life-cycle performance assessment of ship structures under uncertainty", ***Marine Structures***, Vol. 23, No. 3, (2010), 303-321, doi: 10.1016/j.marstruc.2010.07.004.
18. Decò, A., Frangopol, D.M. and Okasha, N.M., "Time-variant redundancy of ship structures", ***Journal of Ship Research***, Vol. 55, No. 3, (2011), 208-219, doi: 10.5957/jsr.2011.55.3.208.
19. Kwon, K. and Frangopol, D.M., "System reliability of ship hull structures under corrosion and fatigue", ***Journal of Ship Research***, Vol. 56, No. 4, (2012), 234-251, doi: 10.5957/JOSR.56.4.100038.
20. Kwon, K., Frangopol, D.M. and Kim, S., "Fatigue performance assessment and service life prediction of high-speed ship structures based on probabilistic lifetime sea loads", ***Structure and Infrastructure Engineering***, Vol. 9, No. 2, (2013), 102-115, doi: 10.1080/15732479.2010.524984.
21. Zayed, A., Garbatov, Y. and Soares, C.G., "Time variant reliability assessment of ship structures with fast integration techniques", ***Probabilistic Engineering Mechanics***, Vol. 32, No., (2013), 93-102, doi: 10.1016/j.probengmech.2013.01.002.
22. Zhu, B. and Frangopol, D.M., "Reliability assessment of ship structures using bayesian updating", ***Engineering Structures***, Vol. 56, (2013), 1836-1847, https://doi.org/10.1016/j.engstruct.2013.07.024.
23. Campanile, A., Piscopo, V. and Scamardella, A., "Time-variant bulk carrier reliability analysis in pure bending intact and damage conditions", ***Marine Structures***, Vol. 46, (2016), 193-228, https://doi.org/10.1016/j.marstruc.2016.02.003.
24. Doshi, K., Roy, T. and Parihar, Y.S., "Reliability based inspection planning using fracture mechanics based fatigue evaluations for ship structural details", ***Marine Structures***, Vol. 54, (2017), 1-22, https://doi.org/10.1016/j.marstruc.2017.03.003.
25. Mansour, A. and Hovem, L., "Probability-based ship structural safety analysis", ***Journal of Ship Research***, Vol. 38, No. 4, (1994), 329-339, https://doi.org/10.5957/jsr.1994.38.4.329.
26. Ayyub, B.M., Assakkaf, I. and Atua, K., "Reliability-based load and resistance factor design (LRFD) of hull girders for surface ships", ***Naval Engineers Journal***, Vol. 112, No. 4, (2000), 279-296, https://doi.org/10.1111/j.1559-3584.2000.tb03337.x.
27. Veritas, D.N., *Fatigue design of offshore steel structures*. 2010, DNV-RP-C203.
28. Mansour, A. and Thayamballi, A., *Probability based ship design; loads and load combinations*. 1993, DTIC Document.
29. Kerdabadi, M.S., Sakaki, A. and Izadi, A., "Evaluation of ship structure reliability during design, maintenance, and repair phases", ***Zeszyty Naukowe Akademii Morskiej w Szczecinie***, (2018).
30. Bowman, M. and Munse, W., "Fatigue behavior of welded steel butt joints containing artificial discontinuities", ***WELDING J.***, Vol. 62, No. 2, (1983), 36.
31. DESIGN, P.B.S., "Ssc-392 probability based ship design: Implementation of design guidelines".
32. Beghin, D., "Fatigue of ship structural details, Society of Naval Architects and Marine Engineers, (2007).
33. Paik, J.K., Kim, S.K. and Lee, S.K., "Probabilistic corrosion rate estimation model for longitudinal strength members of bulk carriers", ***Ocean Engineering***, Vol. 25, No. 10, (1998), 837-860, https://doi.org/10.1016/S0029-8018(97)10009-9.
34. Câmara, M.C. and Cyrino, J.C.R., "Structural reliability applications in design and maintenance planning of ships subjected to fatigue and corrosion", in ASME 2012 31st International Conference on Ocean, Offshore and Arctic Engineering, American Society of Mechanical Engineers., (2012), 503-514.
35. Box, G.E. and Tiao, G.C., "Bayesian inference in statistical analysis, John Wiley & Sons, Vol. 40, (2011).
36. De Haan, L. and Ferreira, A., "Extreme value theory: An introduction, Springer Science & Business Media, (2007).
37. Choi, S.-K., Grandhi, R.V. and Canfield, R.A., "Reliability-based structural design, Springer Science & Business Media, (2006).
38. Devine, E.A., "An overview of the recently-completed jhss monohull and trimaran structural seaways loads test program", Naval Surface Warfare Center, Carderock Division (NSWCCD), PowerPoint Briefing, Vol. 30, (2009).
39. Nikolaidis, E., Ghiocel, D.M. and Singhal, S., "Engineering design reliability applications: For the aerospace, automotive and ship industries, CRC Press, (2007).
40. Mansour, A.E., Wirsching, P., Lucket, M., Plumpton, A., Lin, Y., Jensen, J., Jeom, K.P., Richardson, W., Hess, P. And Hutchison, B., "Structural safety of ships. Discussion. Authors' closure", ***Transactions-Society of Naval Architects and Marine Engineers***, Vol. 105, (1997), 61-98.
41. De Finetti, B. and de Finetti, B., "Theory of probability, volume i", ***Bull. Amer. Math. Soc***, Vol. 83, (1977), 94-97.

Persian Abstract

چکیده

در پژوهش حاضر روند ارزیابی قابلیت اطمینان سازه کشتی تحت دو عامل خرابی خستگی و خوردگی و با استفاده از داده‌های پایش سلامت سازه بیان شده است. به منظور استفاده از داده‌های پایش سلامت سازه در ارزیابی قابلیت اطمینان، از روش استنباط بیزین برای بروز رسانی توزیع بارهای وارد بر سازه استفاده شده است. قابلیت اطمینان سازه یک کشتی تحت عامل خوردگی و با توجه به توزیع بارهای به دست آمده از معادلات، ارزیابی شده است. به منظور استفاده از داده‌های پایش سلامت سازه، از روش استنباط بیزین برای بروز رسانی توزیع بارهای وارد بر سازه استفاده شده است. از خروجی داده‌های سنسورهای نیرویی نصب شده بر روی شناور تجاری در آزمایشگاه که مدل آن بصورت مقیاس تست شده است، جهت بررسی و تحلیل مدل ریاضی پیشنهادی استفاده گردیده است. تحلیل قابلیت اطمینان عیوب خوردگی و خستگی نشان دهنده کاهش شاخص قابلیت اطمینان سازه در طول عمر آن می‌باشد. استفاده از داده های‌پایش سلامت سازه، موجب افزایش اعتماد به شاخص قابلیت اطمینان تخمین عمر واقعی سازه به دست آمده از تحلیل شده است. نتایج نشان می‌دهد با استفاده از معیار قابلیت اطمینان و استفاده از داده‌های پایش سلامت در مرحله طراحی، می¬توان درک بهتری از کارکرد سازه در طول عمر سازه با توجه به شرایط محیطی بدست آورد.